BBA - Molecular Basis of Disease 1865 (2019) 1915–1924

Contents lists available at ScienceDirect

BBA - Molecular Basis of Disease

journal homepage: www.elsevier.com/locate/bbadis

Intracellular cholesterol stimulates ENaC by interacting with phosphatidylinositol-4,5-bisphosphate and mediates cyclosporine A-induced hypertension☆

Yu-Jia Zhai[a,1], Ming-Ming Wu[a,c,1], Valerie A. Linck[a], Li Zou[a], Qiang Yue[a], Shi-Peng Wei[b], Chang Song[a], Shuai Zhang[a], Clintoria R. Williams[a], Bin-Lin Song[a,c], Zhi-Ren Zhang[c,*], He-Ping Ma[a,**]

[a] Department of Physiology, Emory University School of Medicine, Atlanta, GA 30322, USA
[b] Department of Internal Medicine, Medical College of Georgia at Augusta University, Augusta, GA 30912, USA
[c] Department of Cardiology, Clinic Pharmacy, Harbin Medical University Cancer Hospital, Institute of Metabolic Disease, Heilongjiang Academy of Medical Science, Key Laboratories of Education Ministry for Myocardial Ischemia Mechanism and Treatment, Harbin 150081, China

ARTICLE INFO

Keywords:
Cyclosporine A
ABCA1
Aging
PIP_2
ENaC

ABSTRACT

We have previously shown that blockade of ATP-binding cassette transporter A1 (ABCA1) with cyclosporine A (CsA) stimulates the epithelial sodium channel (ENaC) in cultured distal nephron cells. Here we show that CsA elevated systolic blood pressure in both wild-type and apolipoprotein E (ApoE) knockout (KO) mice to a similar level. The elevated systolic blood pressure was completely reversed by inhibition of cholesterol (Cho) synthesis with lovastatin. Inside-out patch-clamp data show that intracellular Cho stimulated ENaC in cultured distal nephron cells by interacting with phosphatidylinositol-4,5-bisphosphate (PIP_2), an ENaC activator. Confocal microscopy data show that both α-ENaC and PIP_2 were localized in microvilli via a Cho-dependent mechanism. Deletion of membrane Cho reduced the levels of γ-ENaC in the apical membrane. Reduced ABCA1 expression and elevated intracellular Cho were observed in old mice, compared to young mice. In parallel, cell-attached patch-clamp data from the split-open cortical collecting ducts (CCD) show that ENaC activity was significantly increased in old mice. These data suggest that elevation of intracellular Cho due to blockade of ABCA1 stimulates ENaC, which may contribute to CsA-induced hypertension. This study also implies that reduced ABCA1 expression may mediate age-related hypertension by increasing ENaC activity via elevation of intracellular Cho.

1. Introduction

Hypercholesterolemia, high plasma Cho, is very common in elderly human beings and acts as a risk factor for cardiovascular diseases. Both hypercholesterolemia and aging are often associated with hypertension. However, it remains unclear how they increase the incidence of hypertension. ENaC plays an important role in maintaining Na^+ homeostasis and controls systemic blood pressure. Gain-of-function mutations of ENaC cause hypertension, as seen in Liddle Syndrome [1–3]. The important role of ENaC in regulating blood pressure has encouraged investigators to determine whether ENaC can be regulated by Cho and account for hypercholesterolemia-induced hypertension. The initial studies show that exogenous Cho and its sequestering agent, methyl-β-cyclodextrin (MβCD), are unable to alter ENaC activity [4,5]. However, Cho in the outer leaflet of the apical membrane of renal epithelial cells is tightly packed with sphingolipids [6,7]. Due to this fact, Cho in the outer leaflet is difficult to be extracted by MβCD or high-density lipoprotein [7,8]. Indeed, we have shown that a relatively high concentration of MβCD is required for MβCD to efficiently extract Cho out of the apical membrane and regulate ENaC [9]. However, it still remains unclear whether the Cho in the outer leaflet is more important for ENaC activity than the Cho in the inner leaflet, because extraction of the outer leaflet Cho may facilitate Cho efflux, resulting in a reduction of the inner leaflet Cho. It is also unknown whether Cho

☆ This article is part of a Special Issue entitled: Genetic and epigenetic regulation of aging and longevity edited by Jun Ren & Megan Yingmei Zhang.

* Correspondence to: Z.-R. Zhang, Department of Cardiology, Clinic Pharmacy, Harbin Medical University Cancer Hospital, Harbin, Heilongjiang 150086, China.
** Correspondence to: H.-P. Ma, Department of Physiology, Emory University School of Medicine, 615 Michael ST, Suite 601, Atlanta GA30322, USA.
E-mail addresses: zhirenz@yahoo.com (Z.-R. Zhang), heping.ma@emory.edu (H.-P. Ma).

[1] These authors contribute equally to this work.

https://doi.org/10.1016/j.bbadis.2018.08.027
Received 30 May 2018; Received in revised form 4 August 2018; Accepted 19 August 2018
Available online 02 September 2018

directly interacts with ENaC or indirectly stimulates ENaC by interacting with other membrane components.

Our recent studies suggest that Cho can regulate the distribution of PIP_2 in the apical membrane to alter the activity of ROMK channels [10]. The apical membrane of epithelial nephron cells contains protrusions called microvilli to increase the surface area for its transporting function. Scanning ion conductance and atomic force microscopy studies suggest that microvilli exist in the distal nephron A6 cells [11,12] and that ENaC may be mainly located in the microvilli [12]. Our previous studies have shown that inhibition of Cho efflux from the inner leaflet of A6 cell apical membrane with ABCA1 inhibitors increases intracellular Cho and ENaC activity [13]. Therefore, Cho may regulate ENaC activity via its inner leaflet localization. It is well known that anionic phospholipids in the inner leaflet of the plasma membrane, especially PIP_2, stimulate ENaC [14–16]. We have shown that the stimulation appears to be caused by a direct interaction between anionic phospholipids and all three ENaC subunits [14,17]. Cho is localized both in the outer leaflet and in the inner leaflet of the plasma membrane. In the outer leaflet, Cho interacts with sphingolipids via hydrogen bonds to form membrane microdomains, also referred as lipid rafts [17–19]. Atomic force microscopy shows that the rafts in artificial membranes exist in a Cho-dependent manner [20,21]. In the inner leaflet, however, it has been suggested that Cho may also interact with PIP_2 to form PIP_2 microdomains or to localize PIP_2 in lipid rafts [22–24]. We have shown that PIP_2 is predominantly localized in microvilli where lipid rafts are located [10]. These studies together indicate that Cho may stimulate ENaC by interacting with PIP_2.

Cho levels in the inner leaflet are precisely controlled by the Cho transporters in the plasma membrane. As a potent Cho transporter, ABCA1 can transport Cho from the inner leaflet to the outer leaflet of the cell membrane [25,26]. A previous report has shown that CsA acts as a potent inhibitor of ABCA1 activity and inhibits ABCA1-mediated Cho efflux in mouse macrophage cell [27]. Our following studies have shown that pharmacological blockade of ABCA1 with CsA elevates intracellular Cho and stimulates ENaC in the distal nephron cells [13], suggesting that increased sodium reabsorption via elevated ENaC activity may account for CsA-induced hypertension. However, it remains unknown whether inhibition of Cho synthesis with statins can attenuate CsA-induced hypertension. In addition, several lines of evidence suggest that impairment of Cho efflux due to reduced ABCA1 function also participates in the pathogenesis of age-related macular degeneration, cardiovascular diseases, and Alzheimer's disease [28–30]. Therefore, elevated ENaC activity due to reduced ABCA1 function may account for the age-related hypertension. In the present study, we show that intracellular Cho stimulates ENaC by promoting the interaction between ENaC and its activator PIP_2 and that this mechanism mediates CsA-induced hypertension. We also show that intracellular Cho is elevated in aging mice due to reduced ABCA1 expression. Therefore, the stimulation of ENaC by intracellular Cho may also account for age-related hypertension.

2. Methods

2.1. Animal use and measurement of systolic blood pressure

All animal protocols and procedures were approved by the Animal Care and Use Committee of Emory University and were conducted in accordance with the Guide for the Care and Use of Laboratory Animals published by the National Institutes of Health. All the animals were purchased from the Jackson Laboratory (Maine, USA). Wild-type C57BL/6 mice were used for a control, whereas apolipoprotein E (ApoE) knockout (KO) mice on a high fat diet were used for producing hypercholesterolemia. For the age-related experiments, both Wild-type C57BL/6 and ApoE KO mice were divided into two groups: aged 3 months as young mice and aged 9 months as old mice. The mice were housed in a temperature-controlled environment (23 ± 2 °C) with a 12-h light/dark cycle. Systolic blood pressure was measured by tail cuff on a warmed platform (BP-2000, Visitech Systems), as previously described [31]. Mice were allowed to rest on the platform for 15 min before measurement. Data from the first 2 days of each blood pressure cycle were discarded as this was considered a transition period in which the mice become accustomed to the procedure. Systolic blood pressure was an average of 3 measurements each day for 4 weeks. To determine the mechanism by which hypercholesterolemia and CsA induce hypertension, ApoE KO mice were randomly divided into 4 groups. The mice were given an intraperitoneal injection of either kolliphor EL (1 ml/kg/day) as a control or CsA (20 mg/kg/day) each day for 4 weeks and fed either normal chow (Rodent Diet 5001; Lab Diet, Brentwood, MO, USA) or high fat diet (TD.06414 Adjusted Calories Diet 60/Fat; ENVIGO, Harlan Laboratories, Madison, WI, USA). To determine the possible effects of lovastatin on CsA-induced hypertension, C57BL/6 mice were randomly divided into four groups and given an intraperitoneal injection each day in each group for 4 weeks: (i) kolliphor EL (1 ml/kg/day) as a control; (ii) CsA (20 mg/kg/day); (iii) CsA (20 mg/kg/day) plus lovastatin (20 mg/kg/day); and (iv) lovastatin (20 mg/kg/day) as another control.

2.2. Cell culture

Xenopus A6 distal nephron cells were purchased from American Type Culture Collection (Rockville, MD) and cultured as we previously reported [32]. The medium contained 2 parts of DMEM/F-12 (1:1) medium (Invitrogen), 1 part of H_2O, 15 mM $NaHCO_3$ (total Na^+ = 101 mM, which is ideal for amphibian A6 cells), 2 mM L-glutamine, 10% fetal bovine serum (Invitrogen), 25 U/ml penicillin, 25 U/ml streptomycin. A6 cells were cultured in plastic flasks in the presence of 1 μM aldosterone at 26 ° C and 4% CO_2. After the cells became 70% confluent in plastic flasks, A6 cells were plated on the polyester membrane of Snapwell inserts (Corning Costar Co) for patch-clamp experiments or Transwell inserts (Corning Costar Co) for confocal microscopy experiments. For imaging using live cells, the cells were cultured on glass coverslip. The cells were cultured for 10 to 14 days to allow them to be fully polarized before each experiment.

2.3. Patch-clamp recordings

Both cell-attached and inside-out patch-clamp recordings of ENaC single-channel currents were carried out using an Axopatch 200B amplifier (Molecular Devices, Sunnyvale, CA). As previously described [13], prior to the experiments, A6 cells cultured on the polyester membrane of Snapwell inserts were thoroughly washed with NaCl solution containing (in mM) 100 NaCl, 3.4 KCl, 1 $CaCl_2$, 1 $MgCl_2$, and 10 HEPES; pH was adjusted to 7.4 with NaOH. The glass micropipette was filled with NaCl solution (the pipette resistance was ranged from 7 to 10 MΩ). Inside-out patches were formed on the apical membrane with the patch pipettes filled with a solution containing (in mM) 100 NaCl, 3.4 KCl, 1 $CaCl_2$, 1 $MgCl_2$, and 10 HEPES. The extracellular solution contained (in mM): 100 KCl, 5 NaCl, 1 $MgCl_2$, and 10 HEPES (50 nM free Ca^{2+} after titration with 1 mM EGTA); pH was adjusted to 7.2 with KOH. To record ENaC single-channel activity in the principal cells, CCD was isolated from mice and split-opened. Cell-attached patches were formed on the apical membrane of the principal cells of split-open CCD, as we previously described [31]. The split-open CCD was bathed in a solution containing (in mM) 140 NaCl, 5 KCl, 1 $CaCl_2$, and 10 HEPES; pH was adjusted to 7.4 with NaOH. The patch pipette was also filled with this solution in which lithium was substituted for sodium (in mM: 140 LiCl, 5 KCl, 1 $CaCl_2$, and 10 HEPES adjusted to pH 7.4 with NaOH). Single-channel currents were obtained with applied pipette potentials of either +40 mV for cell-attached recordings or +60 mV for inside-out recordings, filtered at 1 kHz, and sampled every 50 μs with Clampex 10.2 software (Molecular Devices, Sunnyvale, CA, USA). All experiments were conducted at room temperature (22–24 °C). The total

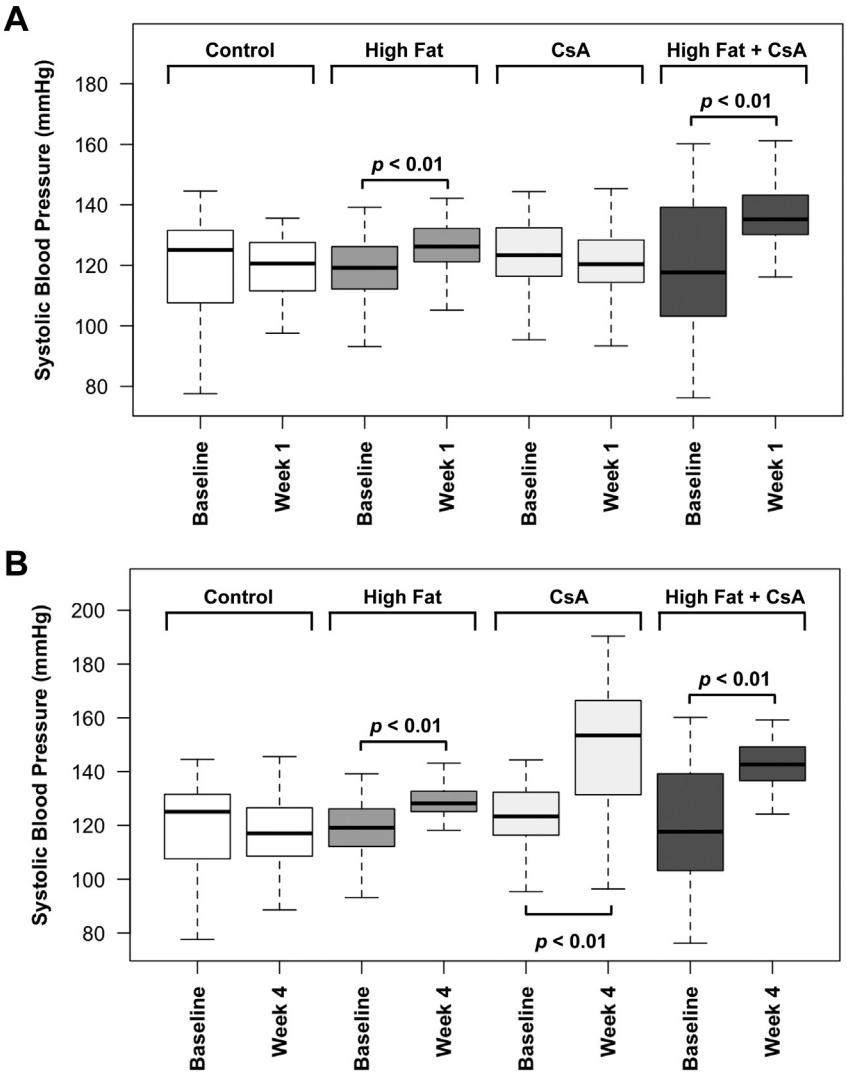

Fig. 1. High fat diet and cyclosporine A (CsA) elevate systolic blood pressure in ApoE KO mice. (A and B) Blood pressure changes in response to high fat diet, CsA, and high fat diet plus CsA either at week 1 (A) or at week 4 (B). 4 mice were used in each group.

numbers of functional channels in the patch were estimated by observing the number of peaks detected on the current amplitude histograms during at least 10 min recording period. Each experiment was started after the first 2-min recordings when the ENaC activity had stabilized. The open probability (P_O) of ENaC, which is percent open time, under control conditions and after each experimental manipulation was calculated using Clampfit 10.2 (Molecular Devices, Sunnyvale, CA, USA).

2.4. Confocal microscopy imaging

Olympus confocal microscope (FV-1000, Japan) was used. Prior to the confocal microscopy experiments, cells were washed twice with saline containing (in mM) 100 NaCl, 3.4 KCl, 1 $CaCl_2$, 1 $MgCl_2$, and 10 HEPES; pH was adjusted to 7.4 with NaOH. To localize α-ENaC in microvilli, A6 cells were fixed with 4% paraformaldehyde for 15 min, permeabilized with 0.1% triton-×100 for 15 min, then incubated with α-ENaC antibody followed with a secondary staining with Alexa Fluor 594 (5 μg/ml). To localize PIP_2 in the microvilli, live A6 cells expressing EGFP-PHD-PLCδ1 on glass coverslip were directly examined by confocal microscope. To analyze γ-ENaC expression, A6 cells were fixed with 4% paraformaldehyde for 15 min, permeabilized with 0.1% triton-×100 for 15 min, then incubated with γ-ENaC antibody (Stressmarq Biosciences) followed with a secondary staining with Alexa Fluor 488 (5 μg/ml). To mark the level of the apical membrane, the cells were also incubated with ZO-1 antibody followed with a secondary staining with Alexa Fluor 594 (5 μg/ml). Confocal microscopy XY scanning of the cells at the apical level was accomplished. For filipin (Cho indicator) staining, frozen kidney sections were fixed in 4% paraformaldehyde and then incubated with 1.5 mg/ml glycine. The kidney sections were incubated overnight at 4 °C with AQP2 antibody and then with Alexa Fluor 594 (5 μg/ml) for 1 h at room temperature. After washing with PBS, filipin was incubated for 1 h at room temperature. Filipin staining was viewed by confocal microscope using DAPI filter.

2.5. Biotinylation and western blot assay

Biotinylation assays of the plasma membrane were performed as described previously [33]. Briefly, after each treatment the A6 cells were incubated with a freshly prepared solution of 1.0 mg/ml EZ-Link sulfo-*N*-hydroxysuccinimide disulfide-biotin (Pierce, Cat. No., 21331) in borate buffer for 30 min at 4 °C. The biotin reaction was quenched for 5 min with 0.1 mM lysine. An equal amount of lysate protein (0.5 mg) from each sample was respectively incubated with 25 μL of immobilized streptavidin-agarose beads (Pierce, Cat. No., 20349) overnight at 4 °C with gentle shaking. The beads were washed four times with RIPA buffer and biotin-labeled proteins were resuspended in 60 μL of Laemmli sample buffer, boiled, and analyzed by Western blot.

2.6. Statistical analysis

Data is reported as mean values ± SE. Statistical analysis was performed with SigmaPlot and SigmaStat software (Jandel Scientific, CA). Student *t*-test was used for comparisons between two groups whereas paired *t*-test was used for comparisons between pre and post treatment activities. Analysis of variance (ANOVA) was used for multiple comparisons among various treatment groups. *Z*-test and chi-squared test were used for comparisons between the changes in percentage. Results were considered significant if $p < 0.05$.

3. Results

3.1. High fat diet and pharmacological blockade of ABCA1 with CsA elevate systolic blood pressure in ApoE KO mice

Hypercholesterolemia is a well-known risk factor for cardiovascular diseases. However, it is unclear whether hypercholesterolemia can induce hypertension. ApoE KO mice on high fat diet have been extensively used as a hypercholesterolemic model. We used this model to test if hypercholesterolemia elevates systolic blood pressure in mice. The data show that high fat diet significantly elevated systolic blood pressure in ApoE KO mice at week 1 (Fig. 1A). We have previously shown that CsA can elevate intracellular Cho and stimulates ENaC in cultured distal nephron cells [13]. Therefore, we also examined the effect of CsA on systolic blood pressure. That data show that CsA did not alter systolic blood pressure in ApoE KO mice at week 1 on normal diet. However, it seems that CsA potentiated the elevation of systolic blood pressure induced by high fat diet (Fig. 1A). CsA even more significantly elevated systolic blood pressure at week 4, even the ApoE KO mice on normal diet. It appears that high fat diet did not induce any additive effect (Fig. 1B). These data suggest that both high fat diet and CsA can elevate systolic blood pressure in ApoE KO mice possibly by sharing the same mechanism.

3.2. Lovastatin attenuates the elevation of systolic blood pressure induced by CsA

Since high fat diet may not always cause hypercholesterolemia, in addition to ApoE KO mice, we also used a mouse model with normal gene expression to determine whether high fat diet can induce hypertension. The data show that high fat diet did not alter systolic blood pressure in C57BL/6 mice (Fig. 2A). However, pharmacological blockade of ABCA1 with CsA to increase intracellular Cho also resulted in a significant increase in systolic blood pressure, and interestingly, the effects was reversed by inhibition of Cho synthesis with lovastatin (Fig. 2B). Since our previous studies have already shown that lovastatin, a Cho synthesis inhibitor, can significantly reduce Cho levels in cultured distal nephron cells [10], these data suggest that intracellular Cho plays a critical role in CsA-induced elevation of systolic blood pressure and that the elevation can be corrected by lovastatin.

3.3. Cho stimulates ENaC in a PIP_2-dependent manner

Our previous studies suggest that CsA stimulates ENaC probably by elevating intracellular Cho [13]. However, the conclusion was dependent on the data from cell-attached patch-clamp experiments with the manipulation of the Cho in the outer leaflet of the cell membrane. To provide direct evidence, here we performed excised inside-out patch-clamp experiments using cultured distal nephron cells. The data show that exposure of the inner leaflet of the patch membrane to only 0.5 mM MβCD significantly reduced ENaC P_O and that the reduction was reversed by 30 μg/ml Cho (Fig. 3A and B). The concentration MβCD we used in this experiment to extract the Cho in the inner leaflet of the apical membrane is 100 times lower than what we previous used (50 mM) to extract Cho out of the outer leaflet [34], suggesting that Cho in the inner leaflet is relatively loose and that the effect of MβCD should be more specific. Since we have recently shown that intracellular Cho plays an important role in concentrating PIP_2, a well-known ENaC activator, we hypothesized that Cho may stimulate ENaC by presenting PIP_2 to ENaC. Indeed, after Cho was extracted out of the inner leaflet of the patch membrane with 0.5 mM MβCD, we used an antibody to PIP_2 to sequester PIP_2 in the inner leaflet of patch membrane. The data show that after ENaC activity was reduced by extraction of Cho in the inner leaflet of the patch membrane with MβCD, addition of Cho no longer reversed the effects when PIP_2 was sequestered with its antibody (Fig. 3C and D). These results suggest that PIP_2 is required for Cho to stimulate ENaC.

3.4. α-ENaC and PIP_2 are localized in microvilli via a Cho-dependent mechanism

By expressing fluorescence-tagged ENaC gene in a cell expression model, we have shown that α-ENaC is co-localized with in microvilli via a Cho-dependent mechanism [35]. Using an ENaC antibody, here we labeled endogenously expressed ENaC in distal nephron cells. First, the cell surface image was obtained with differential interference contrast microscopy (DIC). The image shows that microvilli form a lirelliform structure on the cell surface. Then, by merging the DIC image with the confocal microscopy image of antibody-labeled ENaC, the data clearly show that α-ENaC is localized in microvilli (Fig. 4A). We have recently shown that the ENaC activator PIP_2 is located in microvilli and that its levels are regulated by inhibition of Cho synthesis with lovastatin [10]. Here, again by merging the DIC image with the confocal microscopy image of PIP_2, we show that PIP_2 lined up along with microvilli and that after application of 50 mM MβCD to the same cell, both microvilli and

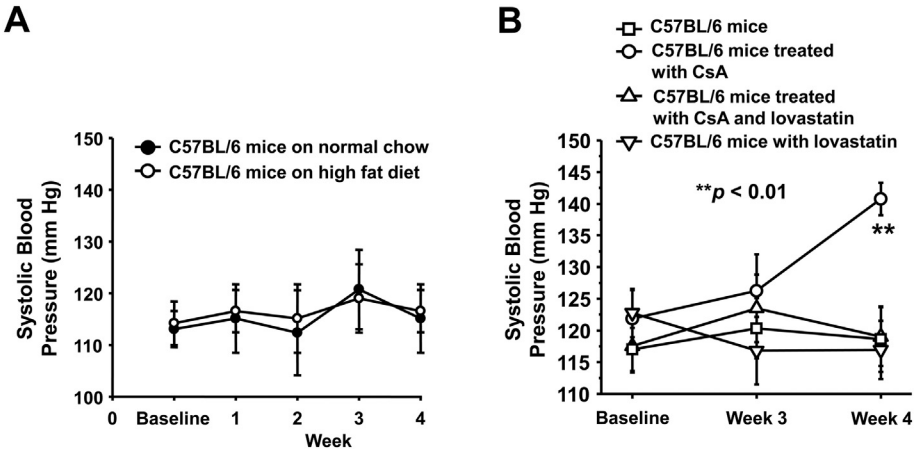

Fig. 2. Lovastatin corrects hypertension caused by loss of ABCA1 function. (A) Systolic blood pressure from mice treated with high fat diet showed no significant difference, compared with wild type C57BL/6 mice. ($n = 9$ in each group). (B) Systolic blood pressure from mice treated with CsA was significantly increased, compared with wild type C57BL/6 mice, while lovastatin attenuated the elevated blood pressure. (**$P < 0.01$ compared with wild type C57BL/6 mice, $n = 8$ in each group).

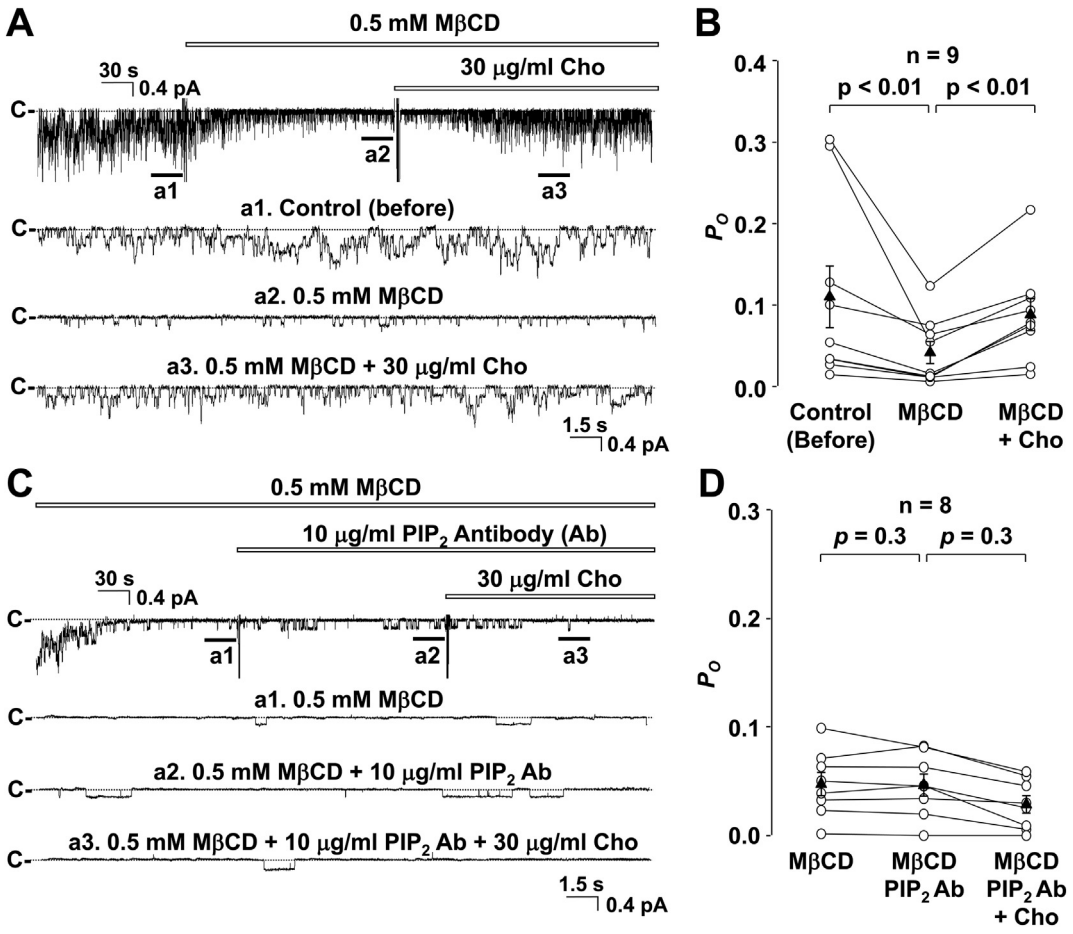

Fig. 3. Cholesterol (Cho) in the inner (cytoplasmic) leaflet of the apical membrane stimulates ENaC via a PIP_2-dependent mechanism. (A) A representative inside-out patch showed that ENaC activity was reduced by addition of MβCD (0.5 mM) into the cytoplasmic bath; the reduction was reversed by addition of Cho (30 μg/ml) into the cytoplasmic bath. "*a1*, *a2*, and *a3*" are zoom-in views of the channel openings (downward events). (B) Summary plots of ENaC P_O under control condition (before), after addition of MβCD, or after addition of Cho in the presence of MβCD to the cytoplasmic bath. Sequestration of PIP_2 with its antibody abolishes the elevation of ENaC P_O by Cho. (C) A representative inside-out patch shows that ENaC activity was reduced after addition of MβCD (0.5 mM) into the cytoplasmic bath; after sequestration of PIP_2 with anti-PIP_2 antibody the reduction was not reversed by addition of Cho (30 μg/ml) into the cytoplasmic bath. "*a1*, *a2*, and *a3*" are zoom-in views of the channel openings (downward events). (D) Summary plots of ENaC P_O after addition of MβCD, after addition of anti-PIP_2 antibody (Ab) in the presence of MβCD, or after addition of Cho in the presence of both MβCD and anti-PIP_2 Ab to the cytoplasmic bath.

PIP_2 were no longer observed (Fig. 4B–D). These data suggest that ENaC is localized in microvilli with PIP_2 that acute extraction of Cho deconstructs microvilli and reduces PIP_2 in microvilli.

3.5. Extraction of Cho with MβCD or inhibition of Cho synthesis with lovastatin reduces γ-ENaC in the apical membrane

To determine whether the ENaC density in or near the apical membrane is regulated by Cho, we labeled γ-ENaC with its antibody. The confocal microscopy images show that extraction of Cho with 50 mM MβCD or inhibition of Cho synthesis with 25 μM lovastatin significantly reduced the levels of γ-ENaC in or near the apical membrane (Fig. 5A and B). To confirm that the reduction occurs in the apical membrane rather than near the apical membrane in the cytoplasm, we also performed biotinylation experiments. The data show that extraction of Cho with 50 mM MβCD or inhibition of Cho synthesis with 25 μM lovastatin did reduce the levels of γ-ENaC in the apical membrane (Fig. 5C). Together with the inside-out patch-clamp results, these data suggest that Cho not only elevates ENaC activity, but also enhances ENaC density in the apical membrane of distal nephron cells.

3.6. Reduced ABCA1 and elevated intracellular Cho in aging mice parallel increased ENaC activity

Recent studies suggest that impaired Cho efflux due to reduced ABCA1 function participates in the pathogenesis of age-related macular degeneration and that mice deficient for ABCA1 demonstrate an accelerated aging phenotype [29]. Our results described above show that loss of ABCA1 function can stimulate ENaC. These studies together suggest that reduced ABCA1 may contribute to the age-related hypertension by stimulating ENaC. Indeed, using a mouse model, here we show that the expression of ABCA1 in the principal cells of CCD was significantly decreased in old mice (9 months), compared to young mice (3 months) (Fig. 6A and B). In parallel to the ABCA1 Cho outwardly transporting function, intracellular Cho was significantly increased in these cells (Fig. 6C and D). Since we have shown that intracellular Cho stimulates ENaC (Fig. 3), ENaC activity in the principal cells of CCD from old mice should be increased. To test this hypothesis, we split-opened the CCD isolated from either young or old mice and performed cell-attached patch-clamp experiments. The data show that ENaC P_O, the number of active channels (N), and NP_O were all increased in old C57BL/6 mice, compared young C57BL/6 mice (Fig. 7A and C). The effects were also observed in ApoE KO mice; it appears that ApoE KO potentiates the increased ENaC P_O, N, and NP_O in old mice (Fig. 7B and

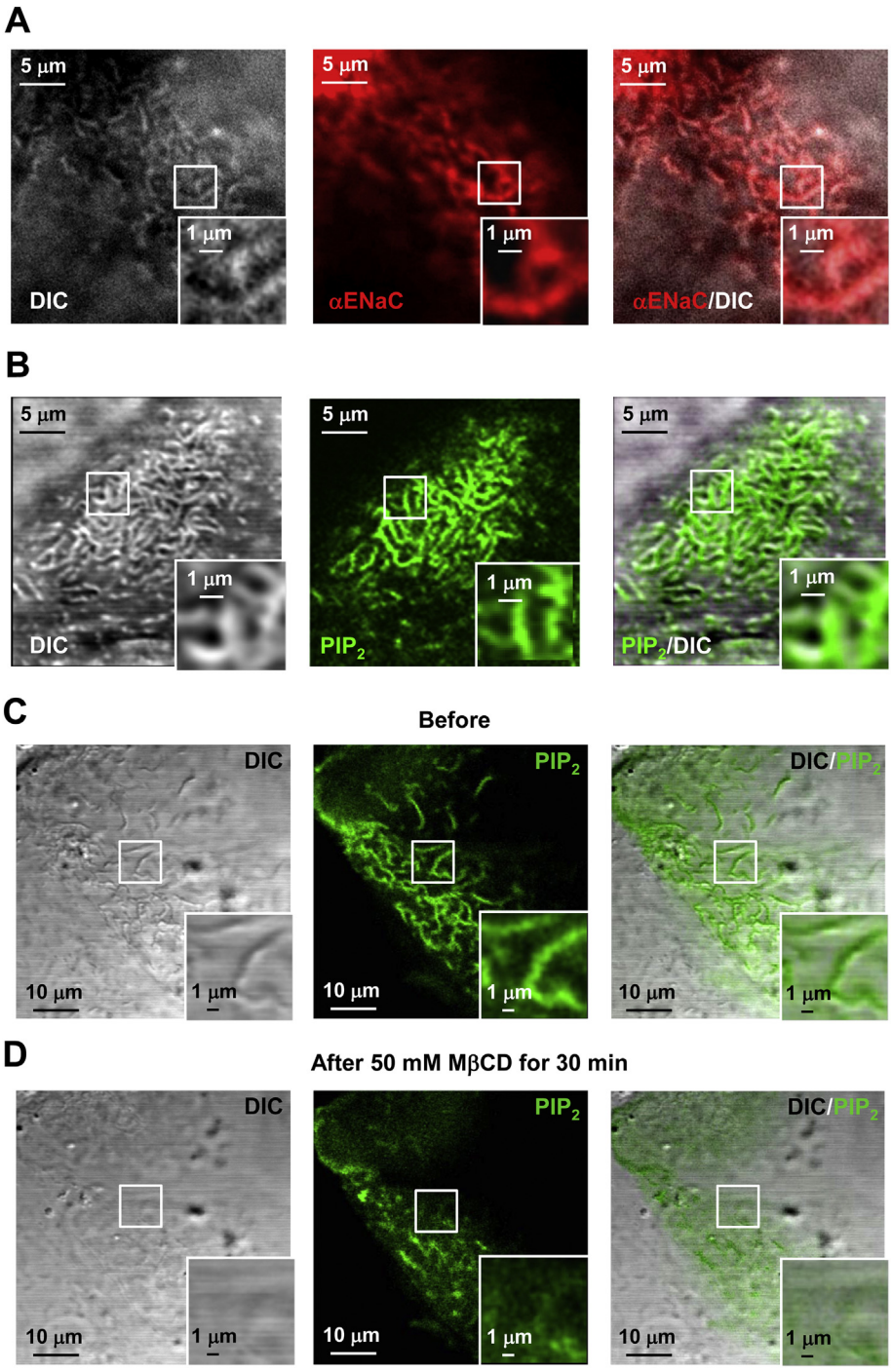

Fig. 4. α-ENaC and PIP_2 are localized in Cholesterol (Cho)-dependent microvilli. (A) Confocal microscopy images show that α-ENaC was localized in microvilli which were clearly seen in DIC and α-ENaC/DIC merged images. The figure represents 7 cells from three experiments showing consistent results. (B) Confocal microscopy images show that PIP_2 was localized in microvilli which were clearly seen in DIC and PIP_2/DIC merged images. (C and D) Confocal microscopy images show that microvilli and PIP_2 in microvilli disappeared after treatment of the cells with 50 mM MβCD for 30 min. The figures in (B) and (C) represent 15 cells from three separate experiments showing consistent results.

C). These data suggest that reduced ABCA1 expression increases sodium reabsorption by stimulating ENaC in the kidney.

4. Discussion

As illustrated in Fig. 8, the present study shows (i) that decreased ABCA1 expression and subsequent increased intracellular Cho occur in aging mice, (ii) that the increased intracellular Cho enhances ENaC activity by promoting the interaction between ENaC and its activator PIP_2, (iii) that the enhanced ENaC activity elevates the blood pressure, and (iv) that pharmacological blockade of ABCA1 with CsA elevates the blood pressure via a Cho-dependent mechanism. These observations together suggest that stimulation of ENaC by intracellular Cho may mediate aging-related and CsA-induced hypertension.

It has long been noticed that immunosuppressant drugs such as CsA and tacrolimus induce hypertension [36,37]. Recent studies suggest that both CsA and tacrolimus cause hypertension by activating the renal sodium chloride cotransporter [38,39]. However, as a calcineurin inhibitor, CsA induces more severe hypertension than tacrolimus [37,40], indicating that other mechanism may be involved for CsA-induced hypertension. Since CsA is not only an inhibitor of calcineurin, but also a blocker of a Cho transporter ABCA1 [41], therefore, using a cultured distal nephron cell line as a model, we have previously shown that blockade of ABCA1 with CsA elevates intracellular Cho and stimulates ENaC [13]. These studies together suggest that CsA may cause hypertension by blocking the Cho-transporting function of ABCA1 to cause accumulation of intracellular Cho in distal nephron cells to stimulate ENaC. Indeed, the present study shows that CsA-induced

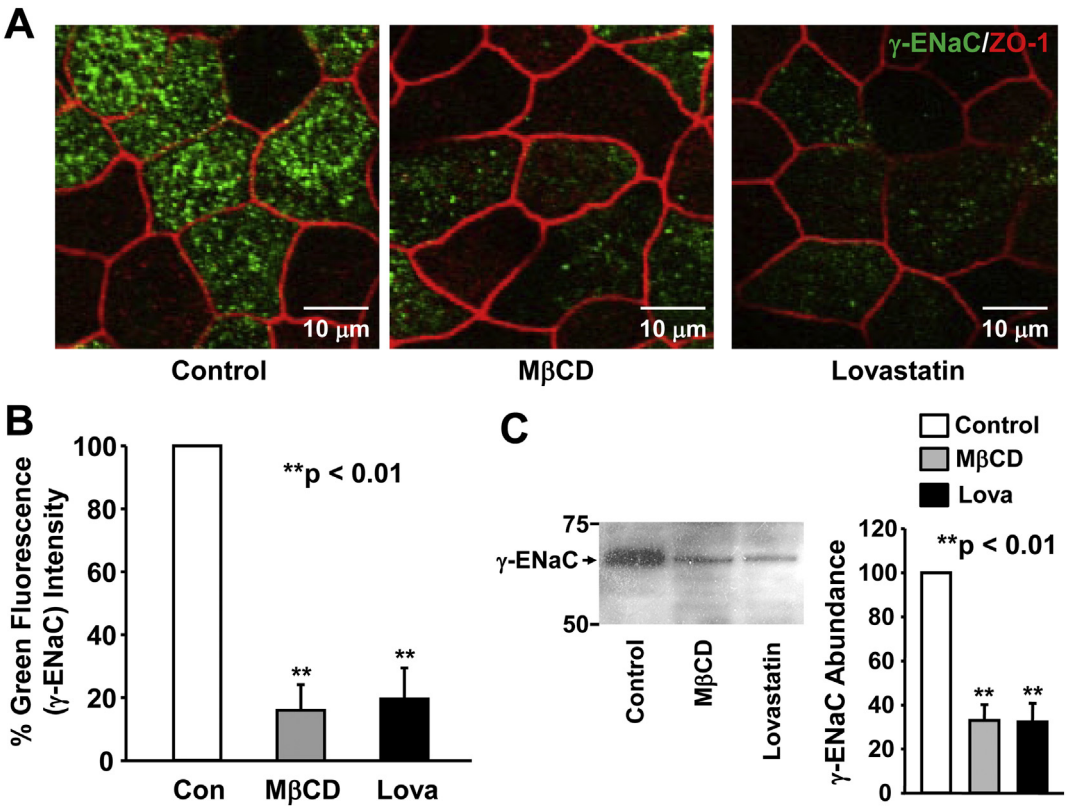

Fig. 5. Extraction of Cholesterol (Cho) and inhibition of Cho synthesis decrease the levels of γ-ENaC in the apical membrane of A6 cells. (A) Confocal microscopy images show that γ-ENaC (shown in green) was significantly reduced either after extraction of Cho with 50 mM MβCD for 30 min or after inhibition of Cho synthesis with 25 μM lovastatin for 24 h. The level near the apical membrane was labeled with a tight junction protein, ZO-1, shown in red. (B) Summary plots of % green fluorescence (γ-ENaC) intensity under each condition. Summary plots represent data from 4 separate experiments. (**$P < 0.01$ compared with control) (C) Western blot of biotinylated apical membrane of A6 cells either under control conditions or treated with 50 mM MβCD for 30 min or 25 μM lovastatin for 24 h. Summary plots represent data from 4 separate experiments. (**$P < 0.01$ compared with control).

hypertension can be corrected by inhibition of Cho synthesis with lovastatin. Although hypercholesterolemia, which is produced by feeding ApoE KO mice a high fat diet, also causes hypertension, it appears not to induce any additive effect on the top of CsA effect. We show that hypertension occurs in ApoE KO mice within one week after on a high fat diet. In contrast, CsA is unable to induce hypertension within the first week, but induces severe hypertension at a later time. This is not surprising, because Cho is mainly synthesized in the liver. In other words, Cho delivery from the blood is the major source for the principal cells to uptake Cho, whereas the Cho synthesis by principal cells themselves is a slow process. However, intracellular Cho accumulation can occur when the expression levels or activity of ABCA1 are reduced, because loss-of-function-mutations of ABCA1 result in Tangier disease by elevating intracellular Cho [42,43].

Our previous studies using the cell-attached patch-clamp technique have shown that it requires a very high concentration of either exogenous Cho (200 μg/ml) or MβCD (50 mM) to respectively stimulate or inhibit ENaC activity [34]. The present study using the inside-out patch-clamp technique shows that MβCD at 0.5 mM, which is 100 times lower than the concentration we used in the cell-attached experiments, significantly reduces ENaC P_O and that the reduction is reversed by 30 μg/ml Cho, which is also > 6 times lower than the concentration we used in the cell-attached experiments. These observations are consistent with the fact that the Cho in the outer leaflet interacts with sphingolipids with long fatty acid chains via hydrogen bonds to form tightly packed microdomains, also referred as lipid rafts [18,28]. Since it is well known that the inner leaflet does not contain any sphingolipids, the Cho in the inner leaflet is unable to be tightly packed to form lipid rafts. Therefore, it requires much less MβCD to extract Cho out of the inner leaflet. Cho in the inner leaflet is known to interact with PIP_2 which is associated with cytoskeleton [44,45]. It is well known that PIP_2 is a strong activator of ENaC. We have shown that anionic phospholipids including PIP_2 can bind to all three ENaC subunits and directly stimulate ENaC in excised inside-out patches [14]. Our recent studies also show that inhibition of Cho synthesis with lovastatin reduces PIP_2 in microvilli [10]. Therefore, PIP_2 might be required for Cho to stimulate ENaC. Indeed, we show that after sequestration of PIP_2 with its antibody, Cho applied to the inner membrane leaflet no longer reverses reduced ENaC P_O caused by extraction of Cho out of the inner membrane leaflet. Furthermore, we show that α-ENaC, a pore forming subunit of ENaC, is co-localized with PIP_2 in the microvilli via a Cho-dependent mechanism. It is known that PIP_2 also promotes protein trafficking [46–48]. Therefore, Cho may also alter ENaC density in the apical membrane by regulating the levels of PIP_2. Indeed, we show that both extraction of Cho with MβCD and inhibition of Cho synthesis can reduce the levels of γ-ENaC, a regulatory subunit of ENaC, in the apical membrane. Since lovastatin could reduce the γ-ENaC expression via inhibition of Cho synthesis, we proposed that lovastatin attenuated hypercholesterolemic and age-related hypertension through inhibiting ENaC activity.

Loss of ABCA1 function is not only due to its mutations, which is rare, and the use of CsA, which is gradually replaced by other immunosuppressive drugs, but is also caused by reduced expression in aging macrophages [29]. The present study for the first time shows that the expression of ABCA1 in the principal cells of aging mouse CCD is reduced and that the intracellular Cho is consistently increased in these aging cells. An age-related increase in Cho accumulation was also found in the mouse kidney [49]. In parallel, our data show that ENaC activity

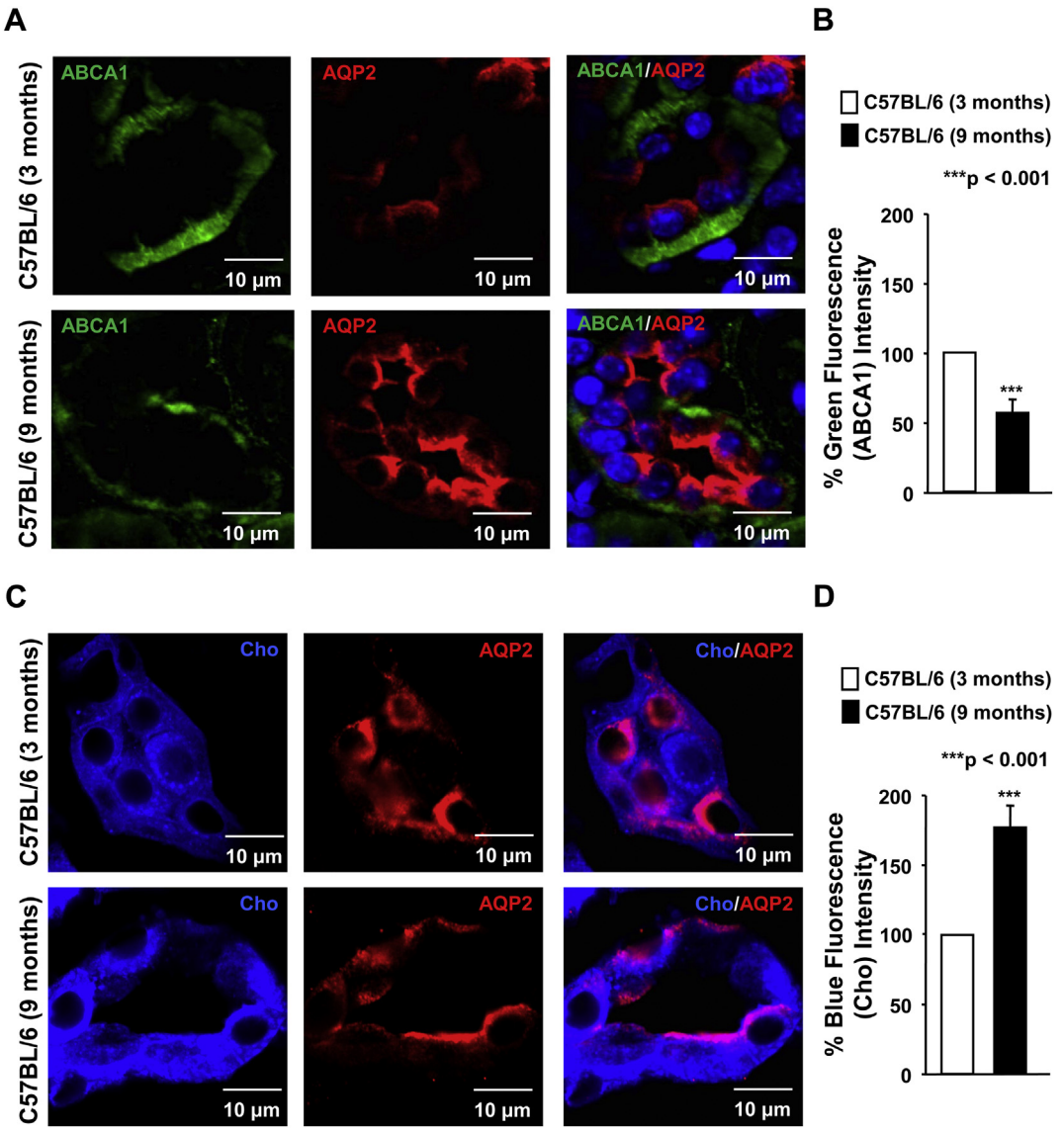

Fig. 6. Decreased ABCA1 expression parallels increased intracellular Cholesterol (Cho) in the CCD of aging mice. (A) Confocal microscopy images of ABCA1 (green) in the principal cells of C57/BL6 mice at either 3 months (upper images) or 9 months (lower images). CCD was labeled with an anti-AQP2 antibody shown in red. The images represent data from 5 mice in each group, showing consistent results. (B) Summary plots of % green fluorescence (ABCA1) intensity. 5 images were used for intensity analysis in each experiment, which was repeated three times in each mouse. (***$P < 0.001$ compared with young mice) (C) Confocal microscopy images of Cho (blue) in the principal cells of C57/BL6 mice at either 3 months (upper images) or 9 months (lower images). CCD was labeled with an anti-AQP2 antibody shown in red. The images represent data from 5 mice in each group, showing consistent results. (D) Summary plots of % blue fluorescence (Cho) intensity. 5 images were used for intensity analysis in each experiment, which was repeated three times in each mouse. (***$P < 0.001$ compared with young mice).

and apical density are also elevated in kidney CCD. Unlike the elevated ENaC activity induced by pharmacological concentration of CsA, which presumably completely blocks ABCA1 function, the elevation of ENaC activity caused by reduced ABCA1 expression can be further increased by hypercholesterolemia, which is known to occur in ApoE KO mice on a high fat diet. It would be interesting to further investigate whether reduced ABCA1 expression participates in age-related hypertension and whether statins can prevent the development of hypertension in aging population.

Transparency document

The Transparency document associated with this article can be found, in online version.

Acknowledgment

The work was supported by grants from Department of Health and Human Services (National Institutes of Health Grant R01-DK100582 to H. M.), Key Project of Chinese National Program for Fundamental Research and Development (973 Program 2014CB542401 to Z.Z.), National Natural Science Foundation of China (81320108002 and 91639202 to Z.Z.), National Natural Science Foundation of China (81600224 to M.W.), National Natural Science Foundation of China (81670381 to B. L.), and Nn10 program of Harbin Medical University Cancer Hospital.

Conflict of interest

None declared.

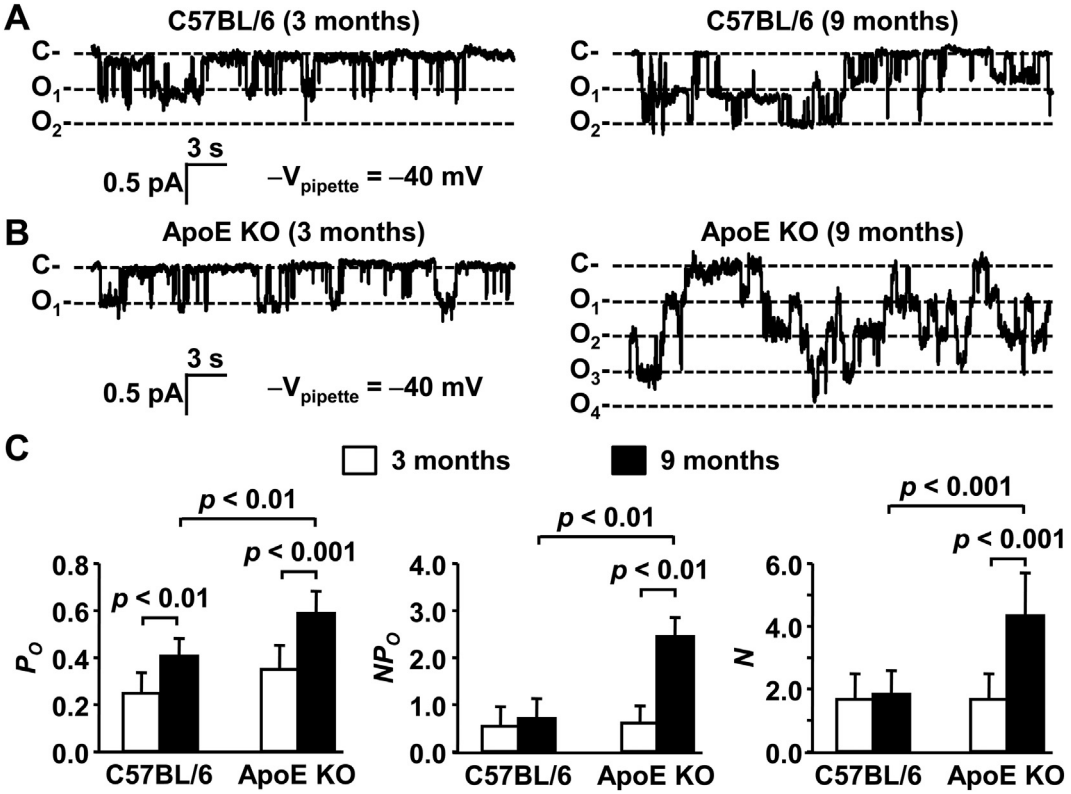

Fig. 7. ENaC activity in the principal cells of the split-open CCD is elevated in aging mice and further increased in ApoE KO aging mice. (A) Representative single-channel recordings from C57BL/6 at either 3 months or 9 months. (B) Representative single-channel recordings from ApoE KO mice at either 3 months or 9 months. Downward events show ENaC openings. $-V_{pipette} = -40$ mV. (C) Summary plots of ENaC P_O, number of ENaC in the patch (N), and NP_O, which is N times P_O. In each experiment, 5 mice were used and 10 cell-attached patches in each group.

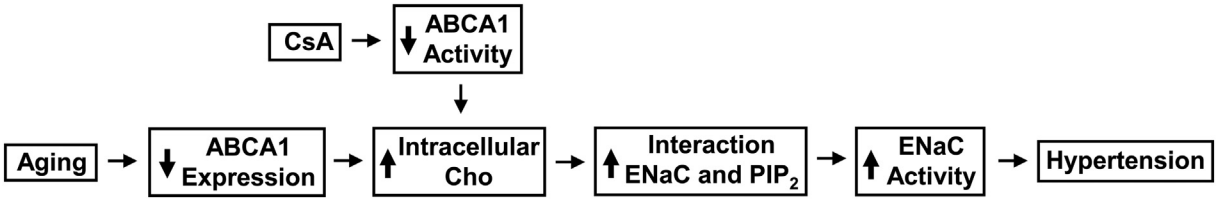

Fig. 8. A schematic diagram describes the role of ENaC in mediating aging-related and cyclosporine A (CsA)-induced hypertension. The underlying mechanism is associated with elevation of intracellular cholesterol (Cho) due to reduced ABCA1 expression.

Author contributions

Yu-Jia Zhai and Ming-Ming Wu: performed research and analyzed data; Valerie Linck, Li Zou, Qiang Yue, Shi-Peng Wei, Chang Song, Shuai Zhang, Bin-Lin Song: performed research; Clintoria Williams: edited the paper; He-Ping Ma, Zhi-Ren Zhang: designed research and wrote the paper; all authors approved the final version of the manuscript.

References

[1] D. Firsov, L. Schild, I. Gautschi, A.M. Merillat, E. Schneeberger, B.C. Rossier, Cell surface expression of the epithelial Na channel and a mutant causing Liddle syndrome: a quantitative approach, Proc. Natl. Acad. Sci. U. S. A. 93 (1996) 15370–15375.
[2] L. Schild, Y. Lu, I. Gautschi, E. Schneeberger, R.P. Lifton, B.C. Rossier, Identification of a PY motif in the epithelial Na channel subunits as a target sequence for mutations causing channel activation found in Liddle syndrome, EMBO J. 15 (1996) 2381–2387.
[3] H. Tamura, L. Schild, N. Enomoto, N. Matsui, F. Marumo, B.C. Rossier, Liddle disease caused by a missense mutation of beta subunit of the epithelial sodium channel gene, J. Clin. Invest. 97 (1996) 1780–1784.
[4] C. Balut, P. Steels, M. Radu, M. Ameloot, W.V. Driessche, D. Jans, Membrane cholesterol extraction decreases Na^+ transport in A6 renal epithelia, Am. J. Physiol. Cell Physiol. 290 (2006) C87–C94.
[5] G. Yue, B. Malik, D.C. Eaton, Phosphatidylinositol 4,5-bisphosphate (PIP2) stimulates epithelial sodium channel activity in A6 cells, J. Biol. Chem. 277 (2002) 11965–11969.
[6] C. Le Grimellec, G. Friedlander, M.C. Giocondi, Asymmetry of plasma membrane lipid order in Madin-Darby Canine Kidney cells, Am. J. Phys. 255 (1988) F22–F32.
[7] A.T. Remaley, B.D. Farsi, A.C. Shirali, J.M. Hoeg, H.B. Brewer Jr., Differential rate of cholesterol efflux from the apical and basolateral membranes of MDCK cells, J. Lipid Res. 39 (1998) 1231–1238.
[8] P. Scheiffele, A. Rietveld, T. Wilk, K. Simons, Influenza viruses select ordered lipid domains during budding from the plasma membrane, J. Biol. Chem. 274 (1999) 2038–2044.
[9] S.P. Wei, X.Q. Li, C.F. Chou, Y.Y. Liang, J.B. Peng, D.G. Warnock, H.P. Ma, Membrane tension modulates the effects of apical cholesterol on the renal epithelial sodium channel, J. Membr. Biol. 220 (2007) 21–31.
[10] B.C. Liu, L.L. Yang, X.Y. Lu, X. Song, X.C. Li, G. Chen, Y. Li, X. Yao, D.R. Humphrey, D.C. Eaton, B.Z. Shen, H.P. Ma, Lovastatin-induced phosphatidylinositol-4-phosphate 5-kinase diffusion from microvilli stimulates ROMK channels, J. Am. Soc. Nephrol. 26 (2015) 1576–1587.
[11] J. Gorelik, Y. Zhang, A.I. Shevchuk, G.I. Frolenkov, D. Sanchez, M.J. Lab, I. Vodyanoy, C.R. Edwards, D. Klenerman, Y.E. Korchev, The use of scanning ion conductance microscopy to image A6 cells, Mol. Cell. Endocrinol. 217 (2004) 101–108.
[12] P.R. Smith, A.L. Bradford, S. Schneider, D.J. Benos, J.P. Geibel, Localization of amiloride-sensitive sodium channels in A6 cells by atomic force microscopy, Am. J. Phys. 272 (1997) C1295–C1298.
[13] J. Wang, Z.R. Zhang, C.F. Chou, Y.Y. Liang, Y. Gu, H.P. Ma, Cyclosporine stimulates

the renal epithelial sodium channel by elevating cholesterol, Am. J. Physiol. Renal Physiol. 296 (2009) F284–F290.
[14] H.P. Ma, S. Saxena, D.G. Warnock, Anionic phospholipids regulate native and expressed epithelial sodium channel (ENaC), J. Biol. Chem. 277 (2002) 7641–7644.
[15] O. Pochynyuk, Q. Tong, J. Medina, A. Vandewalle, A. Staruschenko, V. Bugaj, J.D. Stockand, Molecular determinants of PI(4,5)P_2 and PI(3,4,5)P_3 regulation of the epithelial Na^+ channel, J. Gen. Physiol. 130 (2007) 399–413.
[16] Z.R. Zhang, C.F. Chou, J. Wang, Y.Y. Liang, H.P. Ma, Anionic phospholipids differentially regulate the epithelial sodium channel (ENaC) by interacting with alpha, beta, and gamma ENaC subunits, Pflugers Arch. 459 (2010) 377–387.
[17] H.P. Ma, C.F. Chou, S.P. Wei, D.C. Eaton, Regulation of the epithelial sodium channel by phosphatidylinositides: experiments, implications, and speculations, Pflugers Arch. 455 (2007) 169–180.
[18] K. Simons, E. Ikonen, Functional rafts in cell membranes, Nature 387 (1997) 569–572.
[19] K. Simons, E. Ikonen, How cells handle cholesterol, Science 290 (2000) 1721–1726.
[20] M.C. Giocondi, P.E. Milhiet, P. Dosset, C. Le Grimellec, Use of cyclodextrin for AFM monitoring of model raft formation, Biophys. J. 86 (2004) 861–869.
[21] J.C. Lawrence, D.E. Saslowsky, J.M. Edwardson, R.M. Henderson, Real-time analysis of the effects of cholesterol on lipid raft behavior using atomic force microscopy, Biophys. J. 84 (2003) 1827–1832.
[22] C.M. Johnson, G.R. Chichili, W. Rodgers, Compartmentalization of phosphatidylinositol 4,-bisphosphate signaling evidenced using targeted phosphatases, J. Biol. Chem. 283 (2008) 29920–29928.
[23] J. Maleth, S. Choi, S. Muallem, M. Ahuja, Translocation between PI(4,5)P_2-poor and PI(4,5)P_2-rich microdomains during store depletion determines STIM1 conformation and Orai1 gating, Nat. Commun. 5 (2014) 5843.
[24] J. Wang, D.A. Richards, Segregation of PIP_2 and PIP_3 into distinct nanoscale regions within the plasma membrane, Biol Open 1 (2012) 857–862.
[25] M. Marcil, A. Brooks-Wilson, S.M. Clee, K. Roomp, L.H. Zhang, L. Yu, J.A. Collins, M. van Dam, H.O. Molhuizen, O. Loubster, B.F. Ouellette, C.W. Sensen, K. Fichter, S. Mott, M. Denis, B. Boucher, S. Pimstone, J. Genest Jr., J.J. Kastelein, M.R. Hayden, Mutations in the ABC1 gene in familial HDL deficiency with defective cholesterol efflux, Lancet 354 (1999) 1341–1346.
[26] N. Wang, D.L. Silver, C. Thiele, A.R. Tall, ATP-binding cassette transporter A1 (ABCA1) functions as a cholesterol efflux regulatory protein, J. Biol. Chem. 276 (2001) 23742–23747.
[27] W. Le Goff, D.Q. Peng, M. Settle, G. Brubaker, R.E. Morton, J.D. Smith, Cyclosporin A traps ABCA1 at the plasma membrane and inhibits ABCA1-mediated lipid efflux to apolipoprotein A-I, Arterioscler. Thromb. Vasc. Biol. 24 (2004) 2155–2161.
[28] S.P. Guay, C. Legare, A.A. Houde, P. Mathieu, Y. Bosse, L. Bouchard, Acetylsalicylic acid, aging and coronary artery disease are associated with ABCA1 DNA methylation in men, Clin. Epigenetics 6 (2014) 14.
[29] A. Sene, A.A. Khan, D. Cox, R.E. Nakamura, A. Santeford, B.M. Kim, R. Sidhu, M.D. Onken, J.W. Harbour, S. Hagbi-Levi, I. Chowers, P.A. Edwards, A. Baldan, J.S. Parks, D.S. Ory, R.S. Apte, Impaired cholesterol efflux in senescent macrophages promotes age-related macular degeneration, Cell Metab. 17 (2013) 549–561.
[30] M.J. van Dam, E. de Groot, S.M. Clee, G.K. Hovingh, R. Roelants, A. Brooks-Wilson, A.H. Zwinderman, A.J. Smit, A.H. Smelt, A.K. Groen, M.R. Hayden, J.J. Kastelein, Association between increased arterial-wall thickness and impairment in ABCA1-driven cholesterol efflux: an observational study, Lancet 359 (2002) 37–42.
[31] H.F. Bao, T.L. Thai, Q. Yue, H.P. Ma, A.F. Eaton, H. Cai, J.D. Klein, J.M. Sands, D.C. Eaton, ENaC activity is increased in isolated, split-open cortical collecting ducts from protein kinase Calpha knockout mice, Am. J. Physiol. Renal Physiol. 306 (2014) F309–F320.
[32] H.F. Bao, Z.R. Zhang, Y.Y. Liang, J.J. Ma, D.C. Eaton, H.P. Ma, Ceramide mediates inhibition of the renal epithelial sodium channel by tumor necrosis factor-alpha through protein kinase C, Am. J. Physiol. Renal Physiol. 293 (2007) F1178–F1186.
[33] M.M. Wu, Y.J. Zhai, Y.X. Li, Q.Q. Hu, Z.R. Wang, S.P. Wei, L. Zou, A.A. Alli, T.L. Thai, Z.R. Zhang, H.P. Ma, Hydrogen peroxide suppresses TRPM4 trafficking to the apical membrane in mouse cortical collecting duct principal cells, Am. J. Physiol. Renal Physiol. 311 (2016) F1360–F1368.
[34] A. West, B. Blazer-Yost, Modulation of basal and peptide hormone-stimulated Na transport by membrane cholesterol content in the A6 epithelial cell line, Cell. Physiol. Biochem. 16 (2005) 263–270.
[35] Y.J. Zhai, B.C. Liu, S.P. Wei, C.F. Chou, M.M. Wu, B.L. Song, V.A. Linck, L. Zou, S. Zhang, X.Q. Li, Z.R. Zhang, H.P. Ma, Depletion of cholesterol reduces ENaC activity by decreasing phosphatidylinositol-4,5-bisphosphate in microvilli, Cell. Physiol. Biochem. 47 (2018) 1051–1059.
[36] D.V. Joss, A.J. Barrett, J.R. Kendra, C.F. Lucas, S. Desai, Hypertension and convulsions in children receiving cyclosporin A, Lancet 1 (1982) 906.
[37] T.E. Starzl, J. Fung, M. Jordan, R. Shapiro, A. Tzakis, J. McCauley, J. Johnston, Y. Iwaki, A. Jain, M. Alessiani, et al., Kidney transplantation under FK 506, JAMA 264 (1990) 63–67.
[38] K.I. Blankenstein, A. Borschewski, R. Labes, A. Paliege, C. Boldt, J.A. McCormick, D.H. Ellison, M. Bader, S. Bachmann, K. Mutig, Calcineurin inhibitor cyclosporine A activates renal Na-K-Cl cotransporters via local and systemic mechanisms, Am. J. Physiol. Renal Physiol. 312 (2017) F489–F501.
[39] E.J. Hoorn, S.B. Walsh, J.A. McCormick, A. Furstenberg, C.L. Yang, T. Roeschel, A. Paliege, A.J. Howie, J. Conley, S. Bachmann, R.J. Unwin, D.H. Ellison, The calcineurin inhibitor tacrolimus activates the renal sodium chloride cotransporter to cause hypertension, Nat. Med. 17 (2011) 1304–1309.
[40] V.J. Canzanello, L. Schwartz, S.J. Taler, S.C. Textor, R.H. Wiesner, M.K. Porayko, R.A. Krom, Evolution of cardiovascular risk after liver transplantation: a comparison of cyclosporine A and tacrolimus (FK506), Liver Transpl. Surg. 3 (1997) 1–9.
[41] K. Nagao, M. Maeda, N.B. Manucat, K. Ueda, Cyclosporine A and PSC833 inhibit ABCA1 function via direct binding, Biochim. Biophys. Acta 1831 (2013) 398–406.
[42] M. Bodzioch, E. Orso, J. Klucken, T. Langmann, A. Bottcher, W. Diederich, W. Drobnik, S. Barlage, C. Buchler, M. Porsch-Ozcurumez, W.E. Kaminski, H.W. Hahmann, K. Oette, G. Rothe, C. Aslanidis, K.J. Lackner, G. Schmitz, The gene encoding ATP-binding cassette transporter 1 is mutated in Tangier disease, Nat. Genet. 22 (1999) 347–351.
[43] A. Brooks-Wilson, M. Marcil, S.M. Clee, L.H. Zhang, K. Roomp, M. van Dam, L. Yu, C. Brewer, J.A. Collins, H.O. Molhuizen, O. Loubser, B.F. Ouelette, K. Fichter, K.J. Ashbourne-Excoffon, C.W. Sensen, S. Scherer, S. Mott, M. Denis, D. Martindale, J. Frohlich, K. Morgan, B. Koop, S. Pimstone, J.J. Kastelein, J. Genest Jr., M.R. Hayden, Mutations in ABC1 in Tangier disease and familial high-density lipoprotein deficiency, Nat. Genet. 22 (1999) 336–345.
[44] T. Laux, K. Fukami, M. Thelen, T. Golub, D. Frey, P. Caroni, GAP43, MARCKS, and CAP23 modulate PI(4,5)P_2 at plasmalemmal rafts, and regulate cell cortex actin dynamics through a common mechanism, J. Cell Biol. 149 (2000) 1455–1472.
[45] L.J. Pike, J.M. Miller, Cholesterol depletion delocalizes phosphatidylinositol bisphosphate and inhibits hormone-stimulated phosphatidylinositol turnover, J. Biol. Chem. 273 (1998) 22298–22304.
[46] D.R. Klopfenstein, M. Tomishige, N. Stuurman, R.D. Vale, Role of phosphatidylinositol(4,5)bisphosphate organization in membrane transport by the Unc104 kinesin motor, Cell 109 (2002) 347–358.
[47] T.F. Martin, PI(4,5)P(2) regulation of surface membrane traffic, Curr. Opin. Cell Biol. 13 (2001) 493–499.
[48] A.L. Rozelle, L.M. Machesky, M. Yamamoto, M.H. Driessens, R.H. Insall, M.G. Roth, K. Luby-Phelps, G. Marriott, A. Hall, H.L. Yin, Phosphatidylinositol 4,5-bisphosphate induces actin-based movement of raft-enriched vesicles through WASP-Arp2/3, Curr. Biol. 10 (2000) 311–320.
[49] T. Jiang, S.E. Liebman, M.S. Lucia, J. Li, M. Levi, Role of altered renal lipid metabolism and the sterol regulatory element binding proteins in the pathogenesis of age-related renal disease, Kidney Int. 68 (2005) 2608–2620.